Total Neutron Cross Sections of Sulfur and Tungsten between 5.3 and 6.3 Mev

WEN HUA KAO (高文華), SHIH CHIEN LIN (林世錢), CHANG SUNG LIN (林常松), TZONG-JEN LEE (李崇仁), MING DOU TANG (唐明道), PETER P. Y. MA (馬步原), Yu HAO LEE (李育浩), and JI-PENG CHIEN (錢積彭)

Department of Nuclear Engineering, *National Tsing Hua University, Hsinchu, Taiwan*

(Received September 15, *1967)*

The total cross sections of sulfur and tungsten were measured for neutron energy 5.36-6.28 Mev by the time-of-flight technique. These values were approximated by the sum of the reaction cross sections and the potential scattering cross sections, the latter of which were calculated by this report. It is thus concluded that the compound elastic scattering process is insignificant for both light nucleus, sulfur, and heavy nucleus, tungsten, in this energy range.

I. INTRODUCTION

EXPERIMENTAL results of fast neutron total cross sections with good resolution can provide a detailed knowledge of the resonance structure of the compound nucleus particularly when dealing with light nuclei. Studies of these resonances can lead to informations about spins, total widths, and energy levels of the respective excited states of the compound nucleus. The nuclear radius can be determined from the potential part of the total cross section.

Lane, Langsdorf *et al*[1,2] have studied the total scattering cross sections for sulfur at the energies less than 1.8 Mev, counting all scattering neutrons and integrating $\sigma(\theta)$, and a resonance peak was obtained at the neutron energy 0.59 Mev. Ricamo and Cabe[3] measured the total cross section of sulfur in the energy range 3-5 Mev with several relative maxima and minima presented. The total cross sections for a number of elements, including sulfur and tungsten, have been studied by Nerson and Darden[4,5] for 3.0-15 Mev. Similar measurements have been extended and repeated recently by Glasgon and Foster[6] employing the pulsed-beam time-of-flight method with energy resolution of 2.5%-4.5% for

(1) R. 0. Lane, A. Langsdorf, J. E. Monahan and A. J. Elwyn, Ann. Phys. **12,** 18 (1961), and **12,** 125 (1961).
(2) A. Langsdorf, R. 0. Lane and Monahan, Phys. Rev. **107,** 1077 (1957).
(3) BNL-325 (1958, 1964).
(4) Nerson, Darden, Phys. Rev. 94, 1678 (1954).
(5) N. Nerson, and S. E. Darden, Phys. Rev. **89,** 775 (1953).
(6) Glasgon, Foster, Bull. Am. Phys. Soc. 8, 321 (1963).

$3.0<E_n<15$ Mev. Beyster, Pierre, Machwe, Teach and Tsukada[7,8,9,10,3] studied the elastic and nonelastic cross sections for sulfur and tungsten at a few particular neutron energies with various methods.

In this work, measurements of total cross sections of sulfur and tungsten were repeated with the time-of-flight system of Tsing Hua accelerator. With the help of some particular published values of potential elastic and nonelastic cross sections, the nuclear radius was first calculated and then the potential cross sections were determined as a function of energy in the 5.3-6.3 Mev range. The results show that the total cross section in this region is predominantly composed of potential scattering and reaction cross sections. Then it is also shown that the compound nucleus decays mostly through non-elastic processes because of closely spaced states. This has been found for both light nucleus sulfur and heavy nucleus tungsten.

II. EXPERIMENTAL

(1) Monoenergetic Neutron Source: $D(d,n)^3Me$ reaction

A composite beam with an intensity of **50** μA was produced by the 3-Mev Tsing Hua accelerator. This beam was deflected 25" by an analyzing magnet and reduced to 25μA of deuteron current. After being focussed by a 3" quadrupole lens pair, the analyzed beam passed through the deflecting plates, upon which a potential of 9 Kv *p-p*, 3.5 Mc was applied to chop the beam into pulses with 143 nanosec interval and pulse width of 8 nsec according to the apparatus in use at 2 Mev. Then the pulses went through slits S_1 and S_2. Finally, a **0.4** μA average deuteron beam arrived at the window of the gas target. The whole system is shown in Fig. 1. A current integrator was used to measure the total charge during the course of each run.

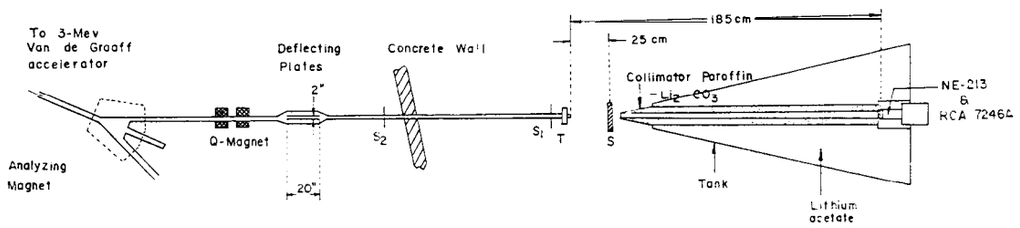

Fig. 1. Schematic Diagram of the Incident Beam and the Shielding System

The gas target as shown in Fig. 2, had a cell of 2.22 cm in length and a window aperture of 1 cm in diameter. To separate the target from the vacuum

(7) Beyster et *al*, Phys. Revs. Rev. 104, 1319 (1956).
Beyster, Henkel, Phys. Rev. 98, 1216 (1955).
(8) St. Pierre, Phys. Rev. **115**, 999 (1959).
(9) M. K. Machwe, Phys. Rev. 114, 1563 (1959).
(10) K. Teach, Nuclear Phys. 37, 412 (1962).

system, a 0.0001" nickel foil was used as the window material which could withstand a presure of two atmospheres. The effective thickness of the foil had an energy loss of 210 Kev.[11] at 3 Mev of deuteron energy. The cell was cooled by a jet of compressed air.

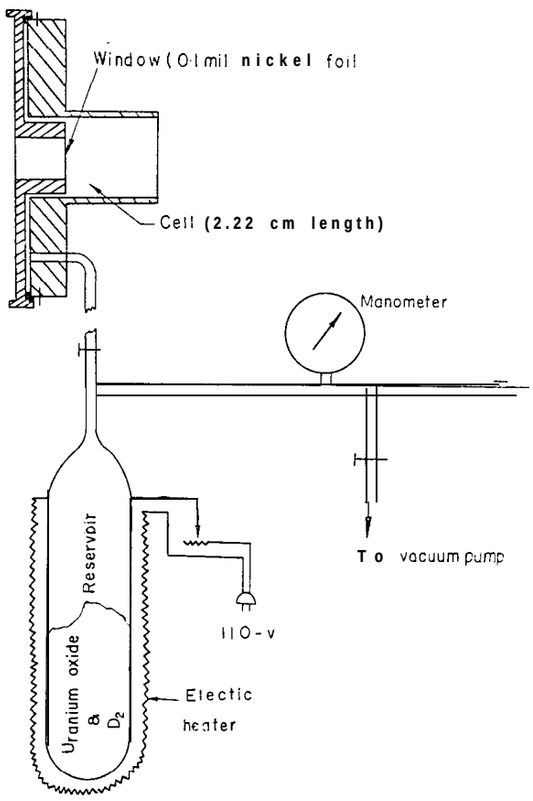

Fig. 2. Gas Target Assembly

Handling of deuterium gas was accomplished with the aid of a reservoir containing uranium oxide which absorbed deuterium gas. The gas pressure was kept at 0.5 atmosphere and indicated by a manometer. The gas thickness was evaluated as 0.10 mg/cm^2, equivalent to 51 Kev[11] at 3 Mev, as the purity of deuterium was 99.7 %.

(2) Detecting System

The detecting system consisted of an NE-213 liquid scintillator, an ***RCA 7264*** photomultiplier tube and the specially designed electronic dircuits. The liquid scintillator shows an effectively longer scintillation decay time for heavily charged

(11) Marion and Fowler, Fast Neutron Phys. Part I, II (1963).

particles such as alphas and protons than for electrons as in Kallmann and Brucker's work[12,13].

As demonstrated by Fig. 3, a signal was picked off by a pickup coil from the rf oscillator for beam deflection. This sine wave was shaped into a square wave to insure minimum zero time uncertainty. After amplification, it was conveyed into the the Time-to-Pulse-Height Converter as the stop pulse.

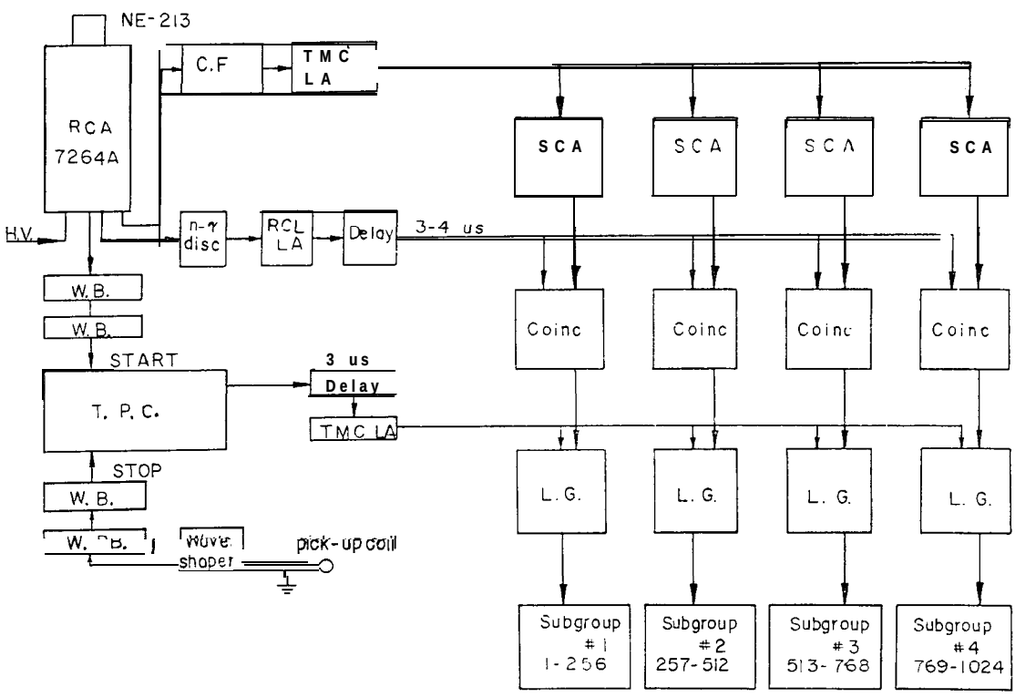

Fig. 3. Block Diagram of the Time of Flight System

The pulses produced in the detector by neutrons and gamma-rays were fed into three different paths. The main one was led out from the anode of the photomultiplier tube into two wide band amplifiers in cascade and then came to the Time-to-Pulse-Height converter as start pulse. The second path was led out combining the 13th dynode and the anode of the phototube for gamma-ray discrimination. A third path was led out from the 11th dynode for linear pulses of recoil protons. When the pulses are divided into four groups, each group has only one quarter of the total time spread effect because of wide variations of recoil proton pulse heights.

(3) Neutron Collimator and Monitor

(12) H. Kallmann and G. J. Bracker. Phys. Rev. 108, 1122 (1957).
(13) F. D. Brocks. Nuclear Instr. and Methods 4, 151-163 (1959).

The detector was placed in a pyramidic iron tank which contained the neutron capture material, lithium hydroxide (LiOH) dissolved in acetic acid with a composition ratio 7:3. When the exothermic reaction had completed, the compound crystallized as lithium acetate. Lithium can capture neuture neutrons without gamma-ray emission and thus reduces the back-ground.

Along the center line of the tank, there was a collimater filled with a mixture of paraffin and lithium carbonate (Li_2CO_3). A 2.5×2.5 cm^2 hole in the collimator provided the flight path for incident neutrons. The solid angle subtended by the detector was only 1.90×10^{-4} steradians at a distance of 185 cm from the target.

Four BF_3 counters embedded in a mixture of Li_2CO_3 and paraffin was employed as the monitor. It was placed below the floor at 90° with respect to the neutron-producing target at a distance about 3 meters from the source. The position and geometry of the surroundings of the monitor collimator was such that the counter looked right upon the neutron source and was not affected by the position of the detector and the sample. It was used to normalize the counting rate at a given neutron energy.

(4) Energy Resolution

The energy resolution corresponding to the beam pulse width and flight path is:

$$E = E_n \frac{2\Delta t}{t} = \frac{2\Delta t}{72.30} E_n^{3/2} \tag{1}$$

where Δt is the time uncertainty, approximately equal to the charged-particle pulse width. D is the flight path in meters, E_n=neutron energy in Mev. t=total flight time. In this work, D=1.85 m, t=8 ns. Then,

ΔE=1.35 Mev (at E_n=5 Mev)

ΔE=1.74 Mev (at E_n=6 Mev)

The energy spread corresponding to the nickel foil and the deutron gas was calculated as E=261 Kev at E_d=3 Mev. Therefore, the overall energy resolution of this work was about 261 Kev.

III. PROCEDURES

In this work, Natural sulfur and tungsten samples were employed for studying. For tungsten, the sample was a solid plate of 5.2 mm in thickness. The sulfur sample (powder) was tightly packed in a thin-walled aluminum container of 7.85 cm in diameter and 1.0 cm in thickness. The density of W, ρ_w is 19.3 gm/cm^3 and that of S, ρ_s=1.723 gm/cm^3.

Procedures of this experiment were as follows:

1) sample-in measurement, 2) sample-out measurement, (an empty container in case of S), 3) background measurement (with 20 cm of lead in place of sample).

For each run, the counting duration was controlled by the neutron monitor and a current integrator which was preset at 20 microcoulombs.

For tungsten sample, all four subgroups in the MCA (1024 channels in total) were used. For sulfur, only a single time spectrum of 256 channels was used without subgrouping for better statistics. Two typical neutron time spectra (257–512 channel) are shown in Fig. 4 for sulfur, and in Fig. 5 for tungsten. In these figures, a) refers to the sample-in run; and b), the sample-out run. There are two peaks in each spectrum corresponding to two charged-particle pulses in each RF cycle. The time separation was 143 ns second ($\frac{1}{2f}=\frac{1}{7}\times10^{-6}=143$ ns). The channel width was $\frac{143}{488-300}=0.76$ ns.

The Total cross section can be calculated from our experimental data and the formula:

$$\sigma=\frac{1}{nd}\ln\frac{\frac{N_0}{M_0}-\frac{B}{M_b}}{\frac{N}{M}-\frac{B}{M_b}}$$

where N, N_0, and B are the counts of sample-in, sample-out and background with the same preset amount of charge on the current integrator; M, M_0 and M_b the counts of monitor respectively. d is sample thickness.

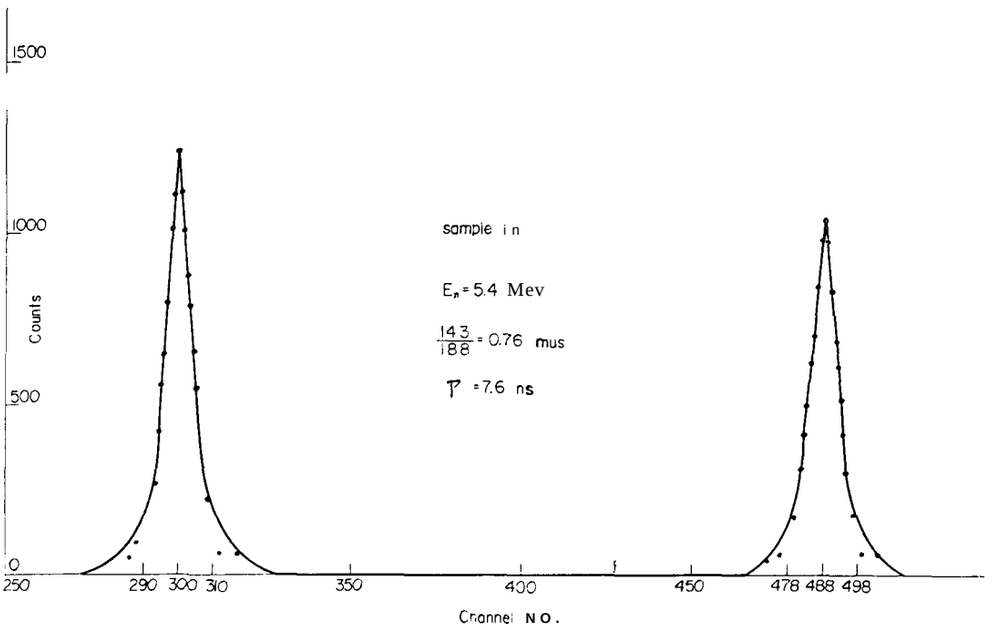

Fig. 4-a. Spectrum of Sulfur

To cover the entire energy range of incident neutron from 5.36 Mev to 6.28 Mev, 40 Kev was used for each step. For each step, three measurements were generally taken for better statistics.

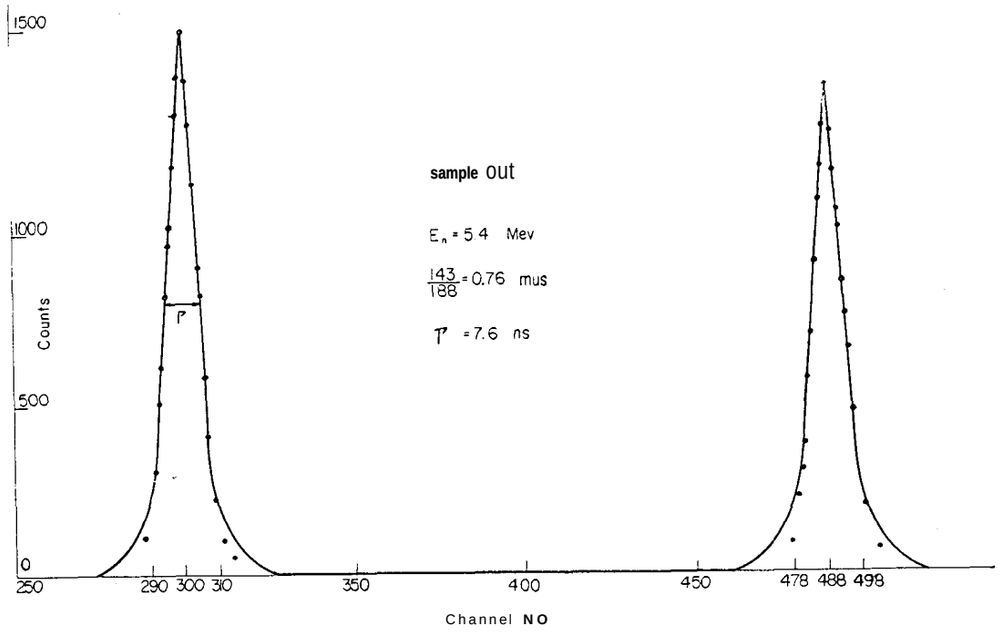

Fig. 4-b. Spectrum of Sulfur

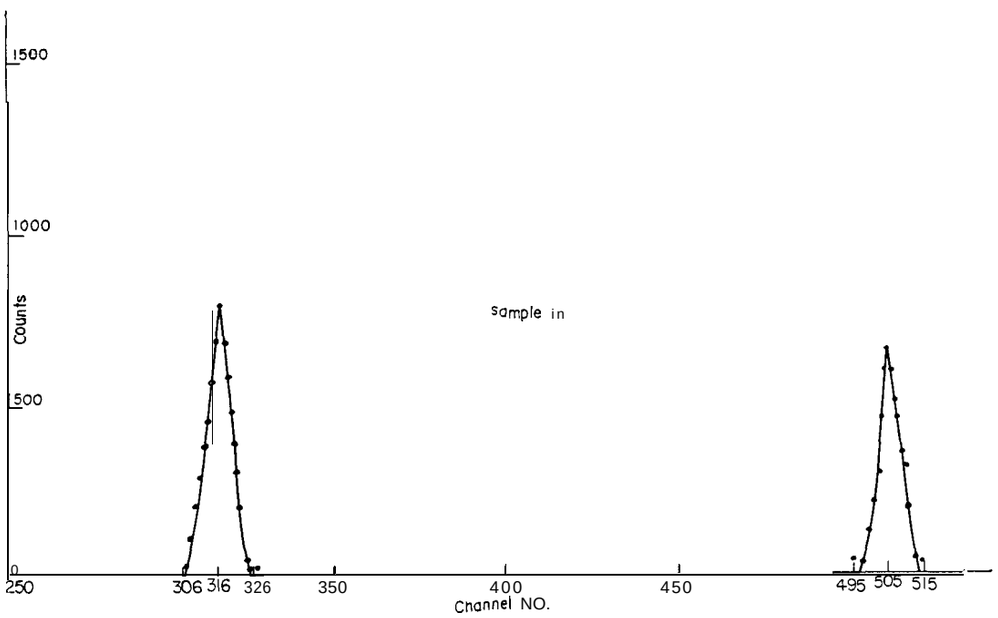

Fig. 5-a. Spectrum of Tungsten

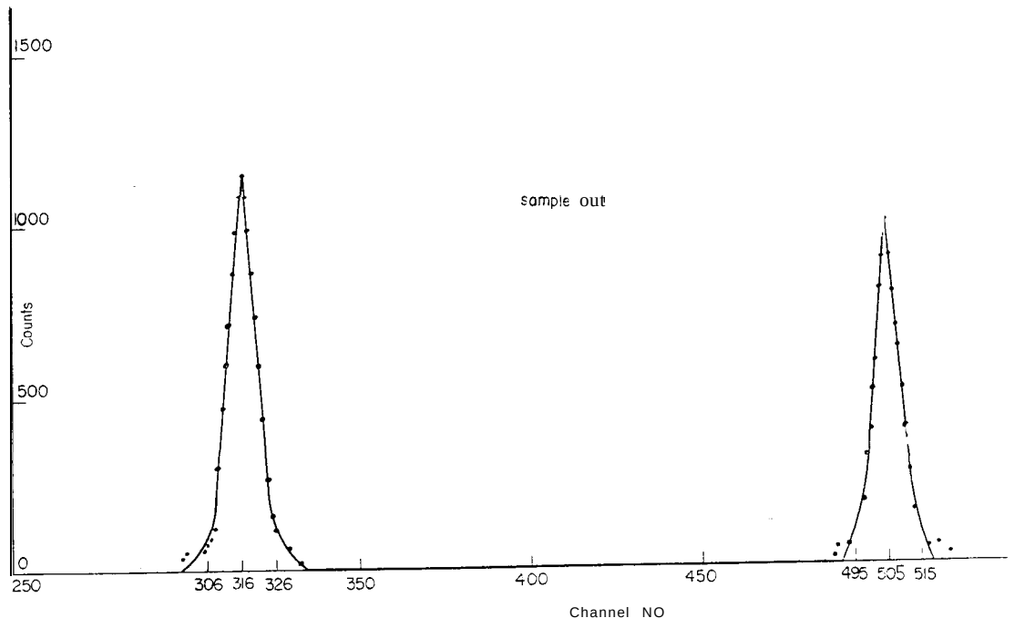

Fig. 5-b. Spectrum of Tungsten

After processing the data, the total cross sections of sulfur and tungsten, as function of incident neutron energy,, are shown in Fig. 6 and Fig. 7 with an error of approximately 11%. In these figures, the potential elastic scattering cross sections were calculated with the knowledge of the compound nuclear radius R determined in the next paragraph.

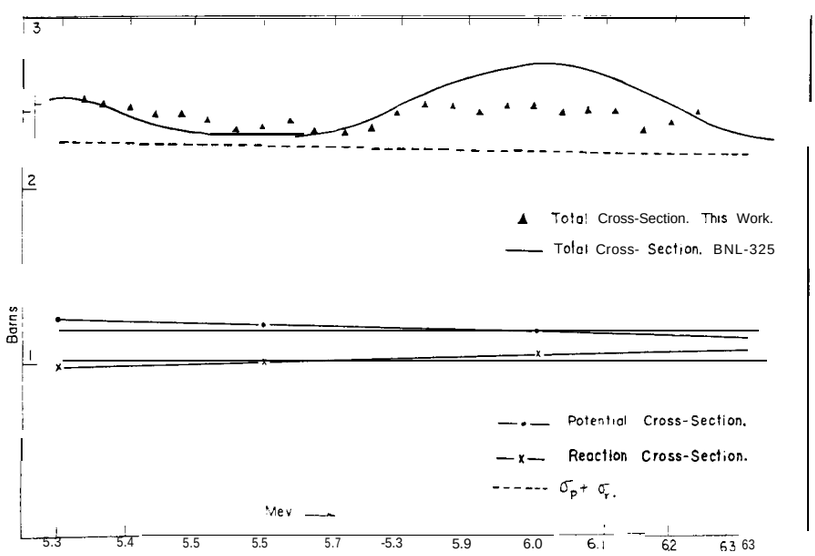

Fig. 6. Total Cross-Section of Sulfur

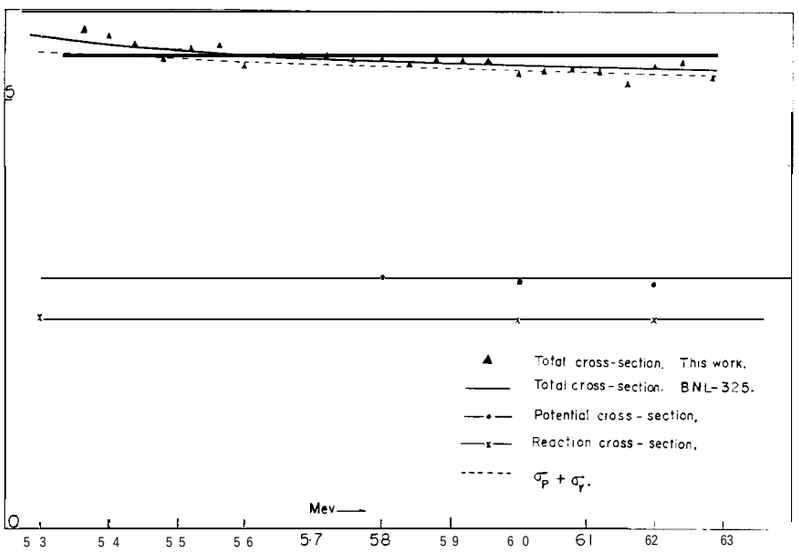

Fig. 7. Total Cross-Section of Tungsten

IV. DATA ANALYSIS

First, the nuclear radius R of sulfur was determined and confirmed with Breit-Wigner formula. With relation $R=r_0A^{1/3}$, the radius of tungsten was also determined. Using the values of R, the potential cross sections as function of energy in the range 5.38-6.28 Mev can be computed. It shows that the total cross section measured in this work is mostly equal to the sum of the potential cross section and the reaction cross sections. Values of the latter were reported by different authors[3,10].

The task to calculate the nuclear radius is based upon the potential cross section :

$$\sigma_p=4\pi\lambda^2\sum_l(2l+1)\ \sin^2\delta_l \tag{3}$$

where $\frac{1}{\lambda}=k=\hbar^{-1}(2M_nE_n)^{1/2}\frac{A}{1+A}\simeq\hbar^{-1}(2M_nE_n)^{1/2}$, $(A=32,\ 184)$. M_n and E_n are the mass and kinetic energy of the incident neutron. δ_l is the phase shift.

The total cross sections, as determmed m this work, consist of potential elastic scattering, compound elastic scattering and nonelastic reaction cross sections. In order to determine the nuclear radius, it is necessary to know the potential fraction of the total cross section.

On the total cross section spectrum S, two minima at 3.85 Mev and 4.2 Mev[3], which may be recognized to consist only of the potential and reaction components, are chosen to determine the nuclear radius R of ^{32}S. The potential scattering cross sections are 1.42 barns and 1.41 barns respectivy, know from the result of

Machwe's work[9] and values of R from 3.0 to 4.4 fm were tried. For each try, the potential cross sections were calculated by the assigned value of R. It has been found that $R=3.83\pm0.04$ fm gives the best results for S.

In the case of tungsten, there is not any suitable point on the energy spectrum representing the favored condition under which the nuclear radius could be cal culated. Here, the relation $R=r_0A^{1/3}$ and the value of r_0 from S (i.e. $r_0=1.19\pm$ 0.012 fm) have been used. Then the radius of W is obtained as

$$R=1.19(185)^{1/3}=6.81\pm0.07 \text{ fm}$$

With the knowledge of R, the neutron energy and Eq. (3), the potential elastic scattering cross section as function of neutron energy are obtained as in Figs. 6 and 7. For S, it ranges from 1.10 to 1.28 barns; and for W, from 2.5 to 3.0 barns.

In the energy range investigated neither sulphur nor tungsten has any clearly spaced resonance peaks appearing so that the single level theory can be applied. But in confirming this value of R, we would like to take the cross section of S at $E_n=590$ Kev as a typical resonance peak.[1,2] It has been known that the resonance cross section is a function of E_n (incident neutron energy), R (nuclear radius), Γ (level width) and other resonance parameters as l (orbital angular momentum), and J (total spin) of the compound system. With the the known values of E_n, R (calculated), and Γ, and the pre-assumed values of resonance parameters, the cross sections were calculated with the help of the IBM-1620 computer. As a resonably good fit between calculations and experimental results the resonance parameters were determined as:

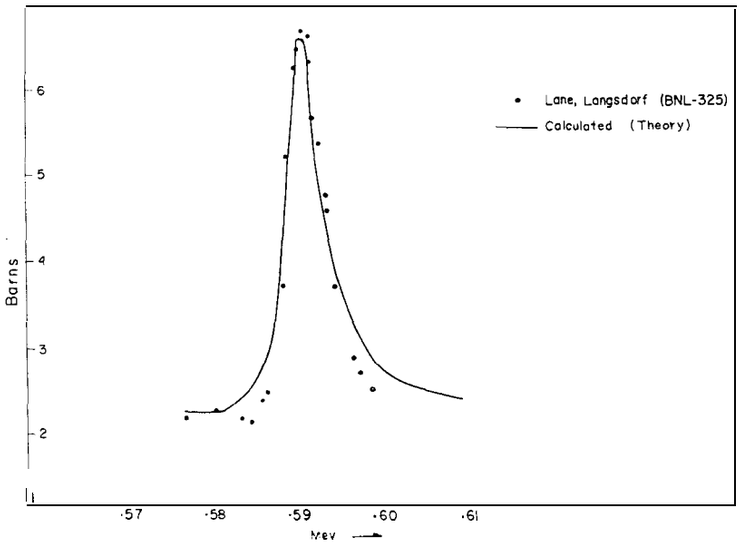

Fig. 8. Total *Cross-Section* of Sulfur

$l=1$, orbital angular momentum,

$J=3/2$, total angular momentum,

Since ^{32}S is an even-even nuclide, conesquently the parity of the compound nucleus is

Π = negative

They are identical with the results of BNL-325. In Fig. 8 at $E_n=590$ Kev, the solid line is the calculated -result with single level formula.

V. DISCUSSIONS

1) Sulfur

The reaction cross sections compiled by BNL-325 cover only some particular values of energy, such as 0.78 barns at 3.7 Mev, 1.14 barns at 7 Mev and 1.14 barns at 14 Mev etc. With the help of these informations and the characteristics that the reaction cross section decreases as the neutron energy

Table I Total Cross-sections of Sulfur and Tungsten (Within 11%)

E_n (Mev)	$t^{(b)}$	
	S	W
5.36	2.52	5.75
5.40	2.49	5.71
5.44	2.47	5.60
5.48	2.43	5.44
5.52	2.43	5.58
5.56	2.40	5.61
5.60	2.35	5.40
5.64	2.36	5.50
5.68	2.38	5.50
5.72	2.33	5.51
5.76	2.32	5.47
5.80	2.34	5.48
5.83	2.42	5.42
5.86	2.47	5.51
5.89	2.46	5.47
5.93	2.43	5.51
5.97	2.47	5.34
6.02	2.47	5.38
6.06	2.42	5.40
6.10	2.43	5.39
6.14	2.42	5.22
6.19	2.31	5.44
6.25	2.37	5.48
6.28	2.41	5.31

increases, here it is shown that the reaction cross section is a function of neutron energy in the region investigated in this work. It is almost as a straight line which may be explainable upon the fact that total cross section of this experimental result is also more or less straight with small fluctuations. If this suggestion is acceptable, the total cross section (result of our work) is compared with the sum of reaction cross section and the potential scattering cross section. The result is that the former is just a little more than the latter. The difference is about 0.2 barn in average and 8% of the total cross section. With this small difference, we can infer that the total cross section in this neutron energy region energy region is predominantly composed of potential scattering and reaction cross sections. If there is any compound elastic scattering cross section at all, it is essentially small and plays no important role i. e. the compound nucleus decays mostly through nonelastic processes.

2) Tungsten :

The reaction cross section as function of neutron energy in the region of 5 to 7 Mev was reported by some others as indicated in BNL-325. The average result was 2.55 $\pm$0.01 barns. The potential scattering cross section determined in section IV was 2.87 to 3 barns. The difference between the total cross section and the sum of the potential scattering and reaction cross section was about 0.13 barns or 3% of the total cross section. The character is similar to that of sulfur.